ADVANCES IN ATMOSPHERIC SCIENCES, VOL. 25, NO. 3, 2008, 447–457

Simulations of the East Asian Subtropical Westerly Jet by LASG/IAP AGCMs

GUO Lanli[1] (郭兰丽), ZHANG Yaocun*[1] (张耀存) WANG Bin[2] (王 斌) , LI Lijuan[2] (李立娟), ZHOU Tianjun[2] (周天军), and BAO Qing[2] (包 庆)

[1] *Department of Atmospheric Sciences, Nanjing University, Nanjing* 210093

[2] *National Key Laboratory of Numerical Modeling for Atmospheric Sciences and Geophysical Fluid Dynamics, Institute of Atmospheric Physics, Chinese Academy of Sciences, Beijing* 100029

(Received 31 January 2007; revised 12 November 2007)

ABSTRACT

Performances of two LASG/IAP (State Key Laboratory of Numerical Modeling for Atmospheric Sciences and Geophysical Fluid Dynamics/Institute of Atmospheric Physics) Atmospheric General Circulation Models (AGCMs), namely GAMIL and SAMIL, in simulating the major characteristics of the East Asian subtropical westerly jet (EASWJ) in the upper troposphere are examined in this paper. The mean vertical and horizontal structures and the correspondence of the EASWJ location to the meridional temperature gradient in the upper troposphere are well simulated by two models. However, both models underestimate the EASWJ intensity in winter and summer, and are unable to simulate the bimodal distribution of the major EASWJ centers in mid-summer, relative to the observation, especially for the SAMIL model. The biases in the simulated EASWJ intensity are found to be associated with the biases of the meridional temperature gradients in the troposphere, and furthermore with the surface sensible heat flux and condensation latent heating. The models capture the major characteristics of the seasonal evolution of the diabatic heating rate averaged between 30°–45°N, and its association with the westerly jet. However, the simulated maximum diabatic heating rate in summer is located westward in comparison with the observed position, with a relatively strong diabatic heating intensity, especially in GAMIL. The biases in simulating the diabatic heating fields lead to the biases in simulating the temperature distribution in the upper troposphere, which may further affect the EASWJ simulations. Therefore, it is necessary to improve the simulation of the meridional temperature gradient as well as the diabatic heating field in the troposphere for the improvement of the EASWJ simulation by GAMIL and SAMIL models.

Key words: East Asian subtropical westerly jet, GAMIL, SAMIL, Diabatic heating

DOI: 10.1007/s00376-008-0447-0

1. Introduction

The East Asian Subtropical Westerly Jet (EASWJ) is a narrow and strong westerly wind belt with large horizontal and vertical shears over the East Asian subtropical region. Previous studies noticed that the seasonal jump of the EASWJ is closely linked to the monsoon climate in East Asia (Yin, 1949; Yeh and Zhu, 1955; Yeh et al., 1958), and the meridional shift of the westerly jet center is associated with the Asian monsoon onset and the interannual variability of the rainfall over East Asia (Lau et al., 1988; Ding, 1992; Liang and Wang, 1998; Li et al., 2004; Zhou and Yu, 2005). Observational studies demonstrate that the seasonal transition of the East Asian general atmospheric circulation pattern and the associated rain band are related to the meridional movement as well as the zonal displacement of the EASWJ (Yeh et al., 1958; Tao et al., 1958; Li et al., 2004; Zhang et al., 2006). Yang et al. (2002) indicated that the EASWJ seems to be linked to the climate signals of Asia and the Pacific region more strongly than ENSO. The decadal shift of the EASWJ is closely related to the rain band shift over the East Asian summer monsoon region. A recent study found

*Corresponding author: ZHANG Yaocun, yczhang@nju.edu.cn

a prominent cooling trend in the upper troposphere around 300 hPa over East Asia during July and August. Accompanying this summertime tropospheric cooling, the EASWJ shifts southward and the East Asian summer monsoon weakens, which results in the tendency toward increased droughts in northern China and flooding along the Yangtze River valley (Yu et al., 2004). The performance of a climate model in simulating the EASWJ is associated with its reproducibility of the East Asian monsoon, but less attention has been paid to this issue. The close relationship between the East Asian monsoon precipitation and the tropospheric jet has provided a good test-bed for climate models (Liang and Wang, 1998; Liu et al., 2001; Zhou and Li, 2002; Zhang and Guo, 2005).

Climate system models have been powerful tools in climate change and variability studies. Many kinds and versions of climate models have been developed by modeling groups throughout the world since the 1980s. The State Key Laboratory of Numerical Modeling for Atmospheric Sciences and Geophysical Fluid Dynamics, Institute of Atmospheric Physics (LASG/IAP) has contributed great efforts to develop comprehensive coupled climate models. Recently a Grid-point Atmospheric Model of IAP/LASG (GAMIL) and a Spectral Atmospheric Model of IAP/LASG (SAMIL) have been developed as the atmospheric component in the climate system models (Wang et al., 2004; Wang et al., 2005a,b). The performances of SAMIL, its early version R15L9 and its coupled model in simulating the climate mean states of atmosphere, land surface, sea ice, and so on, have been evaluated (Liu et al., 1999a,b; Wu et al., 2004a,b; Wang et al., 2005a,b; Zhou et al., 2005a,b; Bao et al., 2006). This indicates that the model is able to simulate the main features of climate mean state and seasonal variations, and that the simulated response to El Niño events are also quite reasonable. However, some large regional biases and uncertainties still exist in the model, and the evaluations on GAMIL are limited (Dai, 2006; Zhou and Yu, 2006). Therefore, more diagnoses and further physical explanations of the model output are necessary for the development of these two models.

The main motivation of this paper is to examine the performances of the LASG/IAP Atmospheric Models GAMIL and SAMIL in simulating the detailed structure and seasonal evolution of the East Asian subtropical westerly jet. Special attention has been paid to the physical interpretation of the biases. The other part of the paper is organized as follows. Section 2 provides a brief description of the model and the data used. Detailed structures and seasonal evolution of the EASWJ and possible influencing factors on the EASWJ simulation are presented in section 3. Concluding remarks are given in section 4.

2. Model and data description

The models used in this paper are the grid-point and spectral atmospheric models developed at LASG/IAP, named GAMIL and SAMIL, respectively. The GAMIL dynamical core designed by LASG/IAP has an adjustable high resolution depending on the available computer's capability and is very stable without any filtering and smoothing. Some important integral properties are kept unchanged, such as the anti-symmetries of the horizontal advection operators and the vertical convection operator, the mass conservation, the effective energy conservation under the standard stratification approximation, and so on (Yu, 1994; Wang et al., 2004). The physical packages of the model are taken from the Community Atmospheric Model Version 2 (CAM2) of the National Center for Atmospheric Research (NCAR) (Kiehl et al., 1996). GAMIL has a $2.8125^\circ \times 2.8125^\circ$ horizontal resolution and 26 vertical layers. The SAMIL model used in this paper is an improved version of the spectral model (Wu et al., 1996), which was developed after its third version truncated at R42 (approximately 2.8125° (lon)$\times 1.66^\circ$ (lat)) horizontal resolution with 26 vertical levels (Wang et al., 2005a,b; Bao et al., 2006). A detailed introduction of the model has been summarized in the reference of Zhou et al. (2005a). For comparison with the NCEP/NCAR reanalysis, all model outputs were interpolated to the horizontal resolution of $2.5^\circ \times 2.5^\circ$.

The sea surface temperature data provided by Atmospheric Model Intercomparison Project (AMIP) from January 1980 to December 1989 were used as boundary conditions to integrate GAMIL and SAMIL for 10 years, respectively. The other data used for comparison with the model results in this paper are monthly mean NCEP/NCAR reanalysis (Kalnay et al., 1996) and the CMAP (Xie and Arkin, 1997) dataset from 1980 to 1989, which represent the observations. The selected meteorological variables of NCEP/NCAR reanalysis data include zonal wind, air temperature, and surface sensible heat flux.

3. Results

3.1 *The horizontal structure of the EASWJ*

Figure 1 shows the simulated and observed zonal wind at 200 hPa in winter (December, January and February) and summer (June, July and August), respectively. In winter, the axis of the observed EASWJ is situated near 30°N and the maximum zonal wind

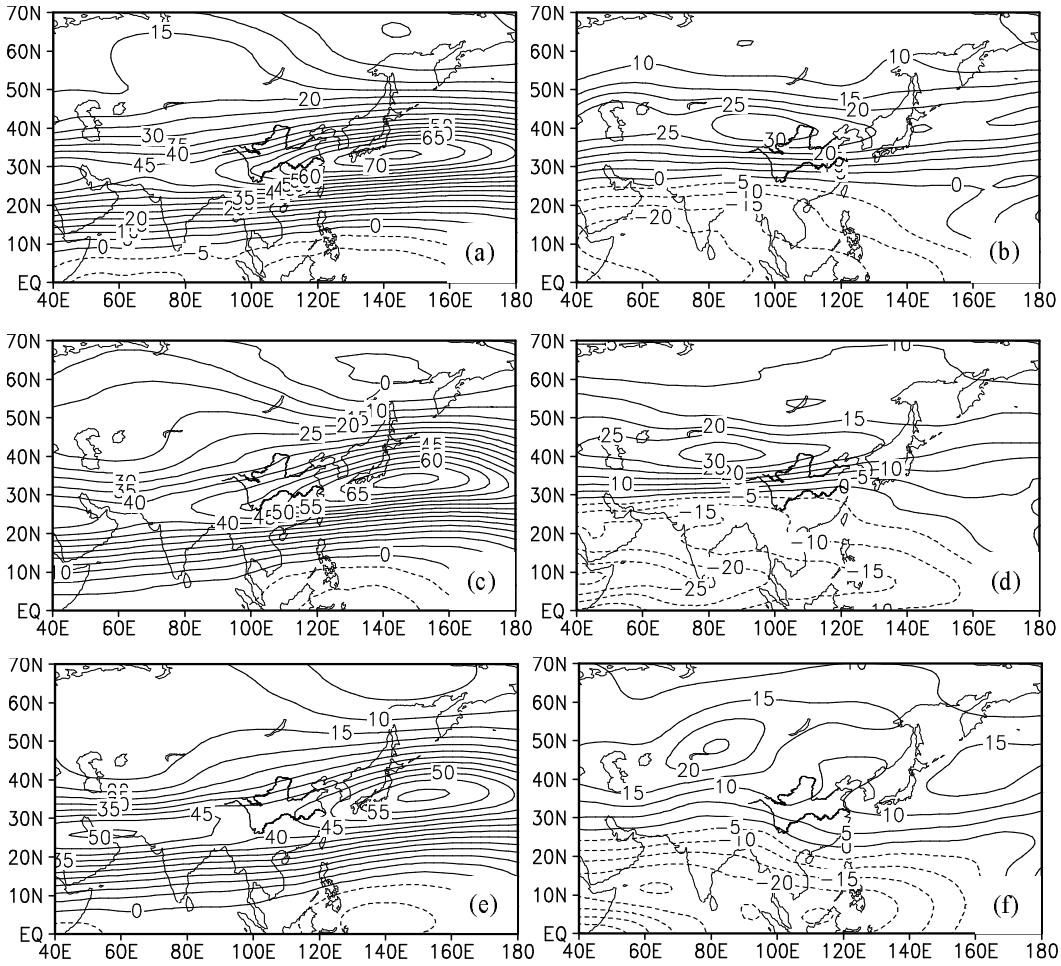

Fig. 1. The zonal wind distributions at 200 hPa in (a, c, e) winter and (b, d, f) summer, respectively. (Units: m s^{-1}) (a, b) Observation, (c, d) GAMIL, (e, f) SAMIL.

speed exceeds 75 m s^{-1} over the ocean to the southeast of Japan. Compared with the observation, the model simulated location of the westerly jet core and the orientation of the jet axis are in good agreement with that observed, but SAMIL reproduces a weaker westerly jet intensity of 60 m s^{-1}, whereas the simulated westerly jet intensity in GAMIL is close to the observation. In summer, the axis of the EASWJ reaches north of 40°N, and the major center of the EASWJ is located over the northern side of the Tibetan Plateau with an intensity of 30 m s^{-1} in the observation. For this season, both models reproduce weaker westerly jet intensities and more northward center locations, especially in SAMIL, with the simulated jet center nearly 10 m s^{-1} weaker than the observation, and the westerly jet obviously shifted westward and northward.

3.2 *The vertical structure of the EASWJ*

Owing to the inhomogeneity of the land-sea and orography distribution, particularly the impact of the Tibetan Plateau on the atmospheric general circulation. Obvious differences exist in the vertical structure of the westerly jet over the different topography (Liang et al., 2006). In order to evaluate the model performance in simulating the westerly jet stream over different regions of East Asia, the latitude-height sections of zonal winds along 90°E, 115°E, and 140°E are presented. The underlying surface is the Tibetan Plateau, flat orography, and ocean, respectively. Figure 2 shows the observed and simulated latitude-altitude sections of the zonal winds along 90°E, 115°E and 140°E in winter. The locations (height and latitude) of the winter westerly jet stream simulated by GAMIL and SAMIL are in good agreement with the observations. The maximum westerly wind occurs between 25°–35°N at 200 hPa. The westerly jet intensity is strongest along 140°E, and becomes weaker gradually westward. Around the Tibetan Plateau the westerly jet core is located on the southern side of the Plateau in winter, and the bifurcation of the jet stream

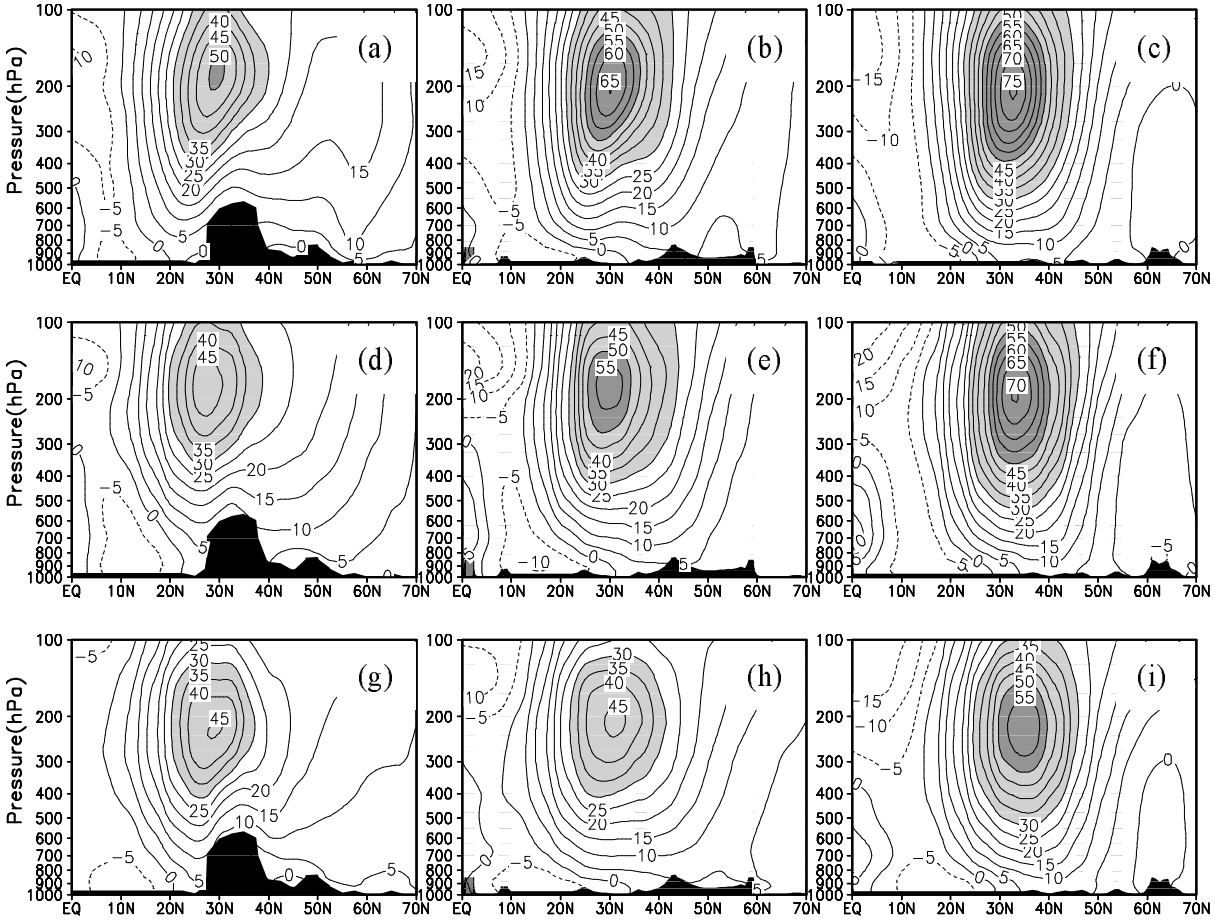

Fig. 2. The latitude-altitude sections of zonal wind along (a, d, g) 90°E, (b, e, h) 115°E and (c, f, i) 140°E in winter, respectively. (Units: m s^{-1}) (a, b, c) Observation, (d, e, f) GAMIL, (g, h, i) SAMIL.

along the two sides of the Plateau at 90°E is well reproduced in GAMIL and SAMIL. But the model simulated southern branches are weaker, and the northern branches are reproduced further south of 40°N. Both models reproduce weaker zonal wind along three longitudes, with westerly jet centers nearly 20 m s^{-1} weaker in SAMIL and about 5 m s^{-1} weaker in GAMIL than that in the observation along 140°E and 115°E, respectively.

Analyses of the simulated and observed zonal winds along 90°E, 115°E, and 140°E in summer, as shown in Fig. 3, indicate that there exist clear deficiencies in the westerly jet simulations. In summer, the most significant feature of the zonal wind is that the westerly intensity is obviously reduced and the westerly jet axis migrates northward to 40°N, while the westerly jet center is located over the northern side of the Tibetan Plateau. Opposite to the case in winter, the wind speed along 90°E is the strongest in the three sections with intensity of 30 m s^{-1} at 200 hPa. Compared with the observations, the model simulations differ obviously from the observation data along these three longitudes, showing 5–10 m s^{-1} weaker westerly jet intensities in the two models. In addition, the simulated locations of the EASWJ shift more northward, especially in SAMIL along 140°E and 115°E.

3.3 *The seasonal evolution of the EASWJ*

In this section, we will present the model performances in reproducing the seasonal evolution of the EASWJ. Figure 4 displays the observed and simulated latitude-time sections of the zonal winds along 90°E, 115°E and 140°E. Along 90°E, the westerly jet center in the observation occurs steadily at 28°N from January to April, and jumps to near 32°N from April to May, then migrates northward to 40°N before retreating southward in August. GAMIL captures the major features of the westerly jet's seasonal evolution along 90°E, but the simulated westerly jet center shifts northward and reaches its northernmost location in September. The SAMIL simulated westerly jet center jumps to 40°N from March to April and moves to the

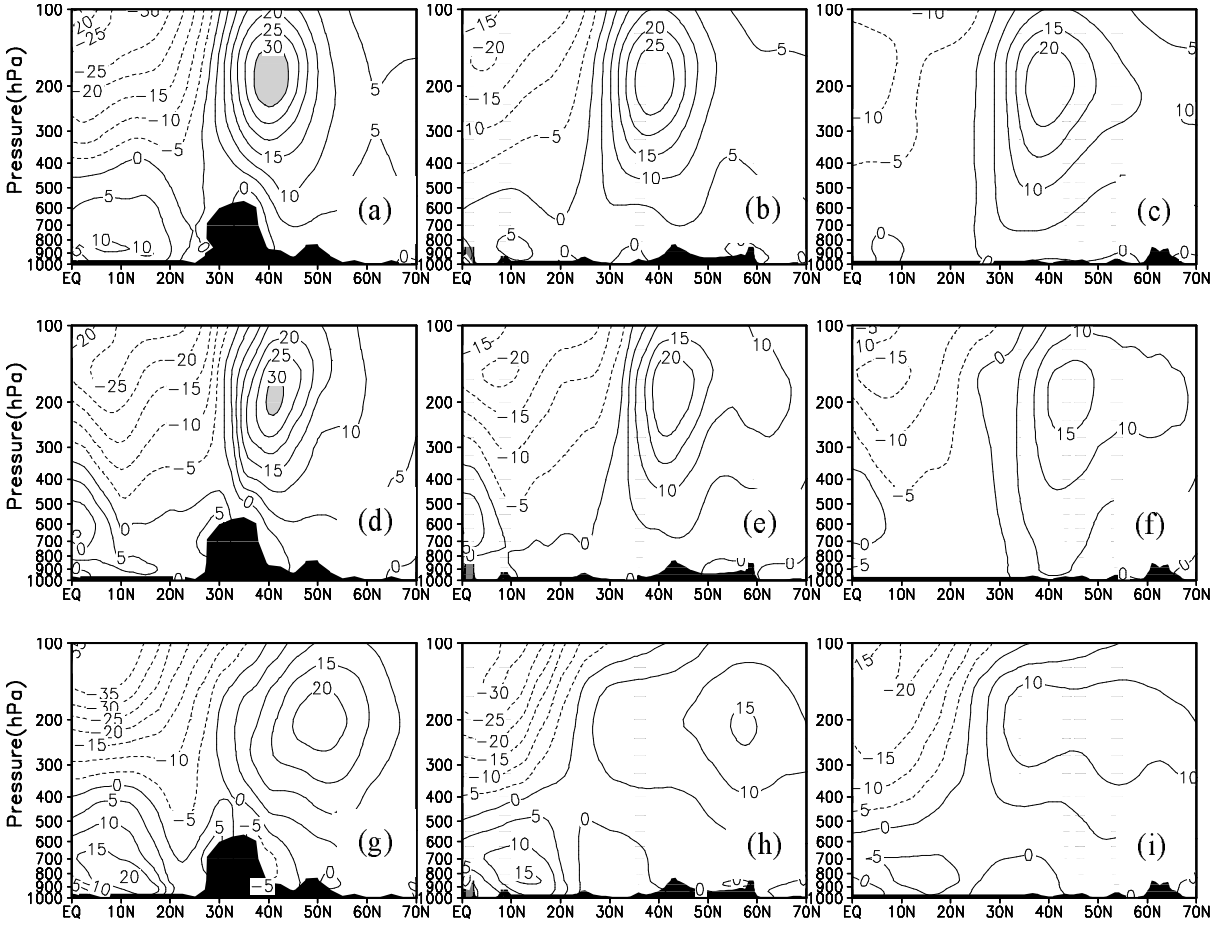

Fig. 3. The latitude-altitude sections of zonal wind along (a, d, g) 90°E, (b, e, h) 115°E and (c, f, i) 140°E in summer, respectively. (Units: m s^{-1}) (a, b, c) Observation, (d, e, f) GAMIL, (g, h, i) SAMIL.

northernmost location near 53°N in July, which is about 10° latitude north of the observation. Along 115°E, the obvious northward jump of the westerly jet center occurs from April to May in the observation, and then the jet migrates northward to 42°N before it's southward retreat in August. The northward jump simulated by GAMIL occurs from March to April, and the simulated westerly jet center moves to the northernmost location in July. For the section along 115°E, the westerly jet center jumps to near 37°N from March to April in SAMIL, and moves northward to 58°N until August, which is about 15° latitude north of that in the observation. Compared with the situations over land, the northward jump along 140°E is not abrupt, where the westerly jet center gradually migrates northward to the northernmost location of 47°N in August, after that it retreats to the winter location. There are two obvious northward jumps from March to April and from June to July in the simulation of GAMIL, and the simulated westerly jet moves to the northernmost location of 52°N in July. There also exist clear discrepancies in the SAMIL simulation, in which the simulated westerly jet is located more northward and jumps to near 56°N from June to July.

The EASWJ seasonal evolution is also reflected by the east-west displacement of the westerly jet center over East Asia. Figure 5 depicts the observed and simulated seasonal evolutions of the EASWJ core in the east-west direction. In the observation, the EASWJ core is located near 140°E before June and at 90°E in July, indicating a rapid westward displacement of the EASWJ core. The core moves to the westernmost location in August, and a rapid eastward retreat occurs from August to September. After that the core retreats around 140°E. Compared with the observation, the simulated longitude location in GAMIL is consistent with the observed result before April, but GAMIL reproduces an early westward movement of the EASWJ core, in which the EASWJ core migrates westward from April, three months earlier than the observed result. In SAMIL, the location shift of the EASWJ core is close to the observation, although

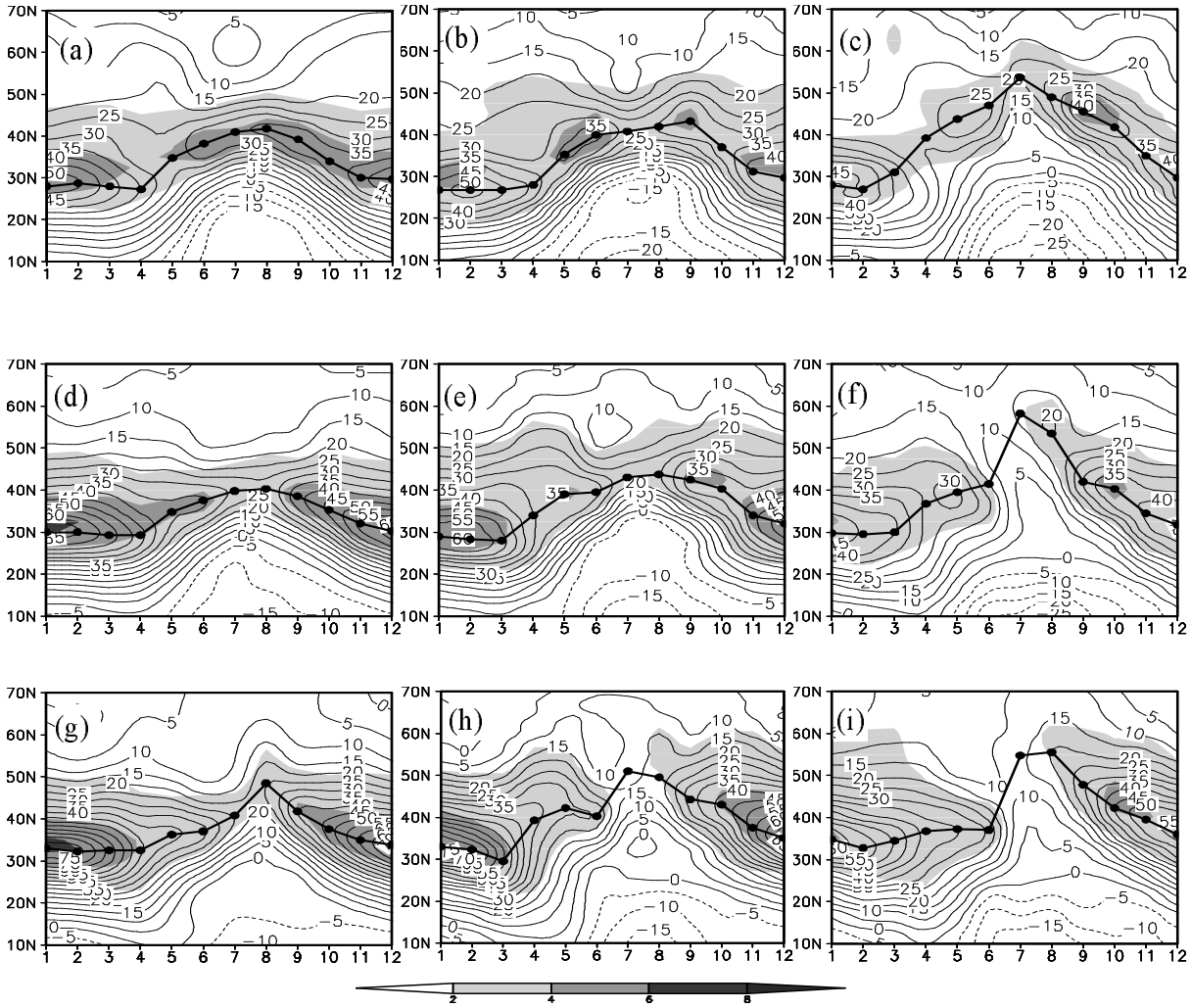

Fig. 4. The latitude-time sections of zonal wind at 200 hPa along (a, b, c) 90°E, (d, e, f) 115°E and (g, h, i) 140°E, respectively. (Units: m s^{-1}) The bold solid line represents the westerly jet axis. The shading is the meridional temperature gradient averaged from 500 hPa to 200 hPa along 90°E, 115°E and 140°E, respectively. [Units: °C(5° lat)$^{-1}$] (a, d, g) Observation, (b, e, h) GAMIL, (c, f, i) SAMIL.

SAMIL does simulate weaker eastward retreat of the EASWJ core in September.

3.4 *The bimodal distribution of the EASWJ in mid-summer*

Figure 6 illustrates the observed and simulated mid-summer occurrence numbers of the westerly jet core from 1980 to 1989. The occurrence number of the westerly jet core is the percentage of the maximum wind speed at each longitude over the region of 20°–70°N and 20°–120°E. In the observation, the large occurrence number of the EASWJ core occurs between 40°–60°E and 80°–110°E in July and August, which is referred to the bimodal distribution of the major EASWJ center in mid-summer. This phenomenon can be found not only in the pentad mean observation data but also in the monthly mean observation data (Zhang et al., 2002). In Figs. 6b and 6c, the occurrence numbers of the EASWJ center in GAMIL and SAMIL occur to the east of 80°E; nearly 80% of the EASWJ cores centralized there. Neither GAMIL nor SAMIL produces an acceptable bimodal distribution of the EASWJ.

3.5 *The possible mechanism*

Based on the principle of the thermal wind, the change in zonal wind with height is largely determined by the meridional temperature gradient. Previous research shows that strong zonal winds normally appear over the frontal area of the troposphere, and that the intensity of the zonal wind is directly proportional to the intensity of the meridional gradient of air tempera-

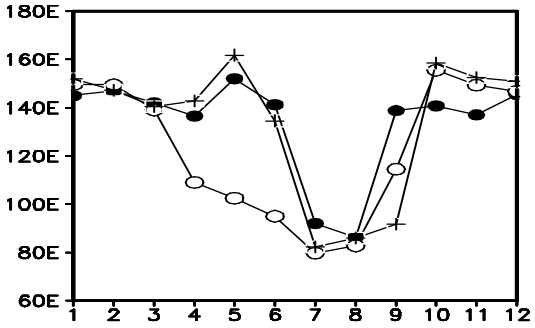

Fig. 5. Seasonal evolutions of the longitude position of the East Asian westerly jet core, in which the solid dot is the observed, the open circle is GAMIL, and the cross is SAMIL.

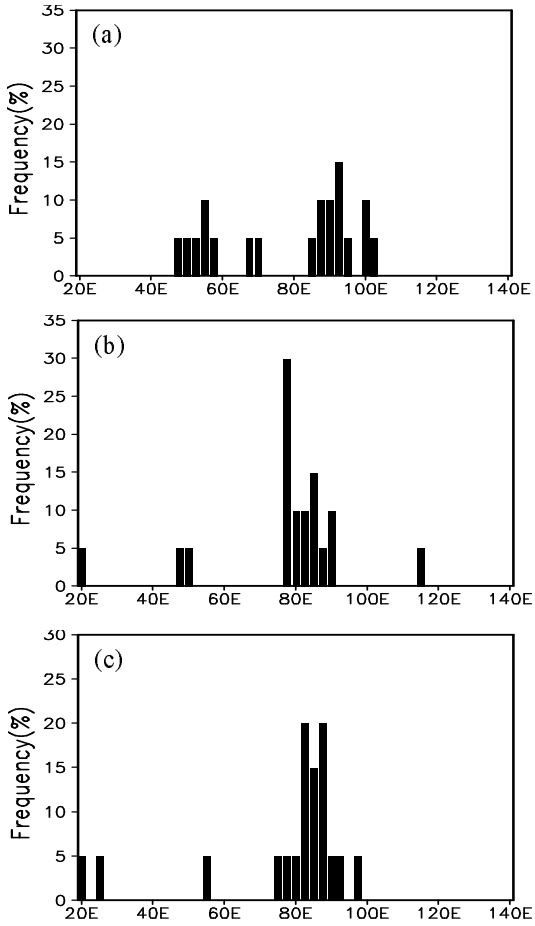

Fig. 6. The occurrence numbers of the westerly center in mid-summer (July and August) from 1980 to 1989. (a) Observation, (b) GAMIL, (c) SAMIL.

ture. The diabatic heating also accounts for the temperature change in the lower-upper troposphere (Kuang and Zhang, 2005). We will analyze the relationship between the seasonal change of the westerly jet core and the meridional temperature gradient in the upper troposphere and the diabatic heating effects on the westerly jet simulation.

The shadings in Fig. 4 are the observed and simulated temporal-latitude variations of the meridional temperature differences averaged from 500 hPa to 200 hPa. The meridional temperature difference which represents the meridional temperature gradient, is calculated by using the air temperature in the south minus that in the north with a 5° latitude interval; positive means relatively warmer in the south and colder in the north. It is shown that the core of the meridional temperature gradients match well with the westerly jet stream, indicating that the seasonal evolution of the westerly jet follows that of the larger meridional temperature gradient in the upper troposphere. As a result, the change of the meridional temperature gradient determines the EASWJ position shift. In the observation, strong meridional temperature gradient occurs in winter, while both models reproduce weaker meridional temperature gradients, leading to a weaker westerly jet in winter. In Fig. 4b and Fig. 4c, the simulated meridional temperature gradients in GAMIL in June and SAMIL in September are larger than that in observation, respectively, leading to a stronger westerly jet. In addition, the simulated maximum meridional temperature gradient occurs most frequently to the east of 80°E in July and August, which accounts for the simulated jet centers being centralized to the east in mid-summer.

The difference in the 500–200 hPa average temperature between the simulations and the observation are presented in Fig. 7. Generally speaking, the simulated winter upper troposphere temperatures in GAMIL and SAMIL are in good agreement with the observation, except that a positive bias appears over the northern parts of the Japan islands in SAMIL. The meridional temperature gradient to the north (south) of the positive temperature difference center will be intensified (weakened). Accordingly, the westerly jet will be intensified (weakened) to the north (south) of positive temperature difference center. In winter, the SAMIL simulated EASWJ core is over the southern part of this positive temperature difference center. Therefore, the weaker westerly jet in SAMIL may result from the simulated warmer upper troposphere over the northern parts of the Japan islands. In summer, there is also a positive bias over northeastern China in GAMIL, and a positive difference center appears near Baikal in SAMIL, which leads to the biases in the westerly jet simulations.

The diabatic heating has a strong impact on the summer atmospheric temperature change over the

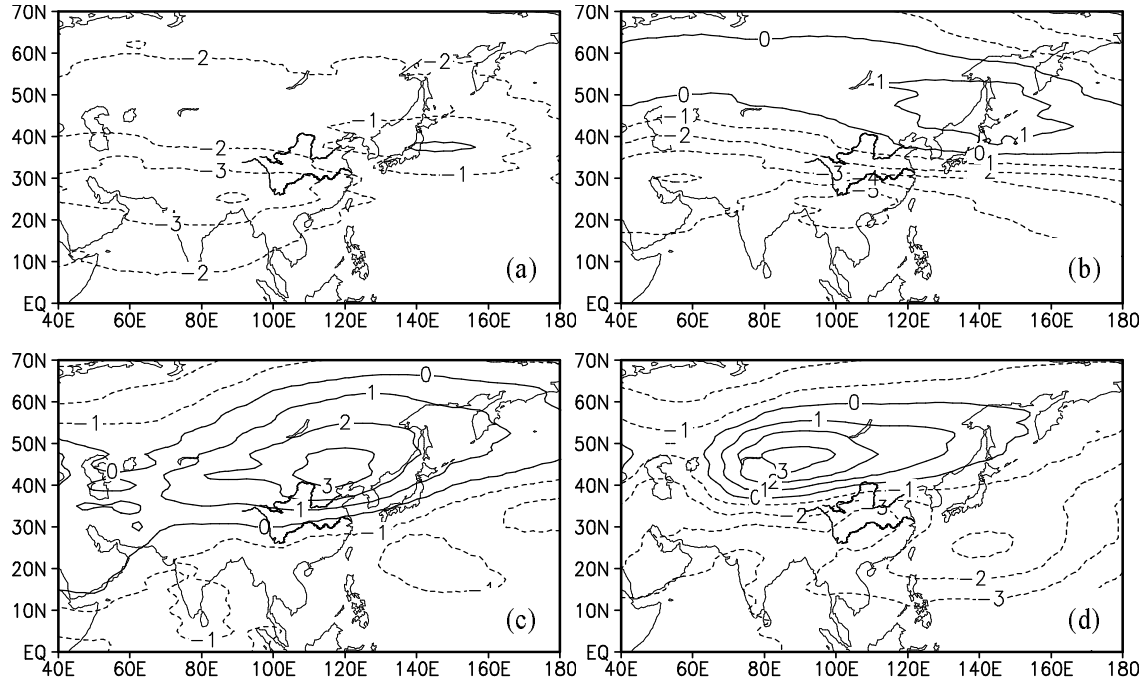

Fig. 7. The differences of the averaged temperature from 500 hPa to 200 hPa between the model simulated and observed in (a, b) winter and (c, d) summer, respectively. (Units: °C) (a, c) GAMIL and Observation, (b, d) SAMIL and Observation.

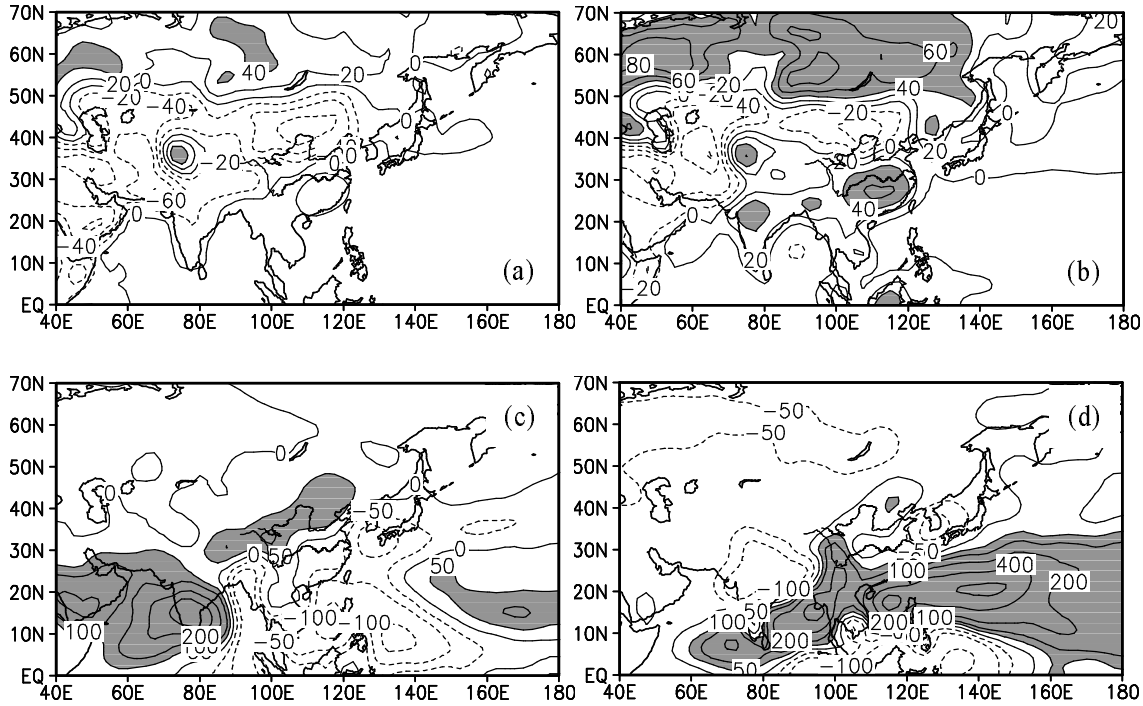

Fig. 8. The differences between the model simulated and observed (a, b) surface sensible heat flux and (c, d) condensation latent heating in summer, respectively. (Units: W m^{-2}) (a, c) GAMIL and observation, (b, d) SAMIL and observation.

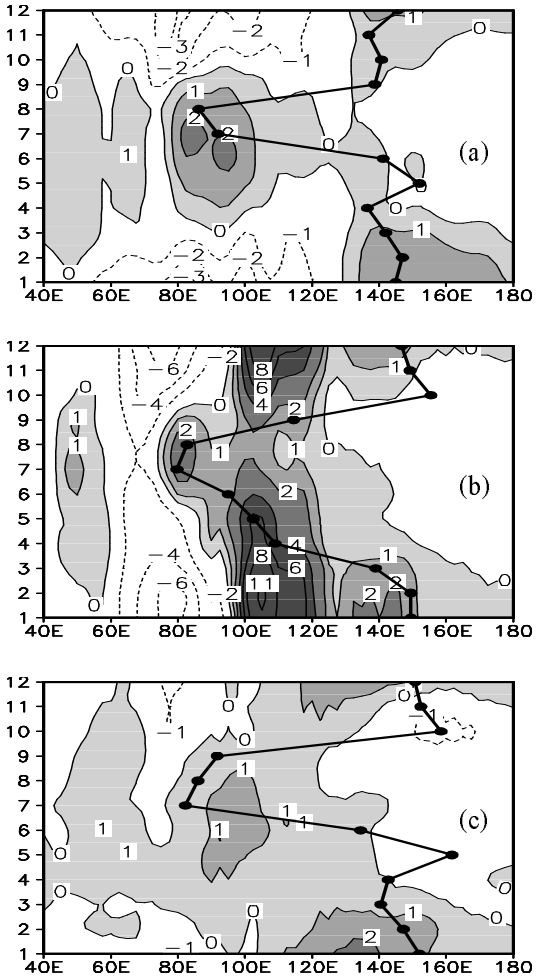

Fig. 9. The longitude-temporal variation of diabatic heating rate averaged between 30°N and 45°N. The dot line represents the westerly jet core locations. (Units: °C d^{-1}) (a) Observation, (b) GAMIL, (c) SAMIL.

Asian continent area from 80°E to 120°E (Wu and Liu, 2003; Liu et al., 2004; Zhang et al., 2006). Figures 8a and 8b show the differences between the simulated and observed surface sensible heat flux in summer, and Figs. 8c and 8d are the differences between the simulated and observed condensation latent heating, which is calculated in terms of the precipitation amount (Yanai et al., 1973). As shown in Fig. 8c, the condensation latent heating in GAMIL is stronger than that in the observation, which matches well with the positive temperature difference center in the upper troposphere (in Fig. 7c) along the Yellow River valley. In Fig. 8b, the surface sensible heat flux in SAMIL is much stronger over the northern parts of the East Asian continent, where the temperature is simulated higher. However, the temperature difference center extends southward from lower-levels to upper-levels. The high surface sensible heat flux area (in Fig. 8b) is to the north of the positive bias of the upper-level temperature (in Fig. 7d). The heating field influences the temperature structure, and results in the changes of the meridional temperature gradient and the pressure field, thus leading to the adjustment of the wind field and the variation of the EASWJ (Kuang and Zhang, 2005).

Figure 9 shows the time-longitude variation of the diabatic heating rate averaged between 30°N and 45°N from surface to 200 hPa. The diabatic heating rate is computed from the thermodynamics equation, which includes turbulent heating, condensation heating and radiative heating rates. In the observation, the strong heating rate is located to the east of 130°E before May, and the westerly jet core occurs over this area coincidently. With the enhancement of the heating rate from 80°E to 100°E, the jet core approaches this area. Meanwhile, the heating rate to the east of 120°E weakens. Thus the diabatic heating rate is responsible for the intensity change and location shift of the westerly jet in the upper troposphere. The models capture the major seasonal evolution features of the diabatic heating rate, but have apparent discrepancies in the simulated results. A much stronger heating rate center exists between 100°E and 120°E from September to the following June in GAMIL, which corresponds to the westerly jet center located westward from April to September. In SAMIL, the heating rate is also stronger to the west of 130°E. These discrepancies may affect the model simulation on the seasonal evolution of the westerly jet.

4. Concluding remarks

In this paper, the performances of the LASG/IAP AGCMs in simulating the EASWJ have been evaluated. The key points are summarized below:

(1) GAMIL and SAMIL can reasonably simulate the winter westerly jet, but the simulated summer westerly jet is located further to the north and the simulated intensity weakens obviously, especially in SAMIL.

(2) In SAMIL, the simulated westerly jet extends more northward, and the times when the westerly jet jumps northward and when the westerly jet reaches its northernmost location do not match the observations along 90°E, 115°E and 140°E.

(3) For the east-westward migration of the westerly jet core, the two models reproduce early westward movement of the EASWJ cores, especially GAMIL, in which the EASWJ core migrates westward from April, three months earlier, whereas SAMIL simulates later EASWJ core eastward retreat in September.

(4) The GAMIL and SAMIL simulated jet cen-

ters centralize near 80°E in mid-summer, thus the phenomenon of the bimodal distribution of the major EASWJ center can not be reproduced in the models.

The simulated meridional temperature gradient is weaker than that in the observation, particularly in SAMIL. This may be the reason for the weaker simulated westerly jet. In addition, the maximum meridional temperature gradients in GAMIL and SAMIL always occur to the east of 80°E in July and August, which result in the simulated jet centers centralized east in mid-summer. The condensation latent heating over northeastern China is stronger in GAMIL, and the surface sensible heat flux is much stronger over the northern part of the East Asian continent in SAMIL, which are responsible for the temperature simulation, and further influence the westerly jet simulation over this area. Apparent discrepancies exist in the simulated time-longitude variation of the diabatic heating rate, which may affect the intensity change and location shift of the westerly jet.

The LASG/IAP Atmospheric Models (GAMIL and SAMIL) possess the ability to simulate the major features of the EASWJ. The discrepancies are probably related to the inappropriate calculation of the surface sensible heat flux or other diabatic heating such as the atmospheric radiation and convective condensation heat release in the models. Moreover, the performances of the other atmospheric models in simulating the East Asian westerly jet need to be evaluated in the following work. The current analysis has provided a good test-bed or observational metric for the validation of AGCMs over East Asia.

Acknowledgements. The reanalysis data was provided by the National Centers for Environmental Prediction (NCEP) and National Center for Atmospheric Research (NCAR). This work was jointly supported by the National Natural Science Foundation of China under Grant No. 40675041, and Open Research Program of State Key Laboratory of Atmospheric Sciences and Geophysical Fluid Dynamics (LASG), Institute of Atmospheric Physics, Chinese Academy of Sciences. We also appreciate insightful comments and suggestions from the two anonymous reviewers

REFERENCES

Bao, Q., Y. M. Liu, T. J. Zhou, Z. Z. Wang, G. X. Wu, and P. F. Wang, 2006: The sensitivity of the spectral atmospheric general circulation model of LASG/IAP to the land process. *Chinese J. Atmos. Sci.*, **30**(6), 1077–1090. (in Chinese)

Dai, A. G., 2006: Precipitation characteristics in eighteen coupled climate models. *J. Climate*, **19**(18), 4605–4630.

Ding, Y. H., 1992: Summer monsoon rainfalls in China. *J. Meteor. Soc. Japan.*, **70**, 373–396.

Kalnay, E., and Coauthors, 1996: The NCEP/NCAR 40-year reanalysis project. *Bull. Amer. Meteor. Soc.*, **77**(3), 437–471.

Kiehl, J. T., and Coauthors, 1996: Description of the NCAR Community Climate Model (CCM3). NCAR Tech. Note NCAR/TN-420+STR, 152pp.

Kuang, X. Y., and Y. C. Zhang, 2005: Seasonal variation of the East Asian subtropical westerly jet and its association with the heating field over East Asia. *Adv. Atmos. Sci.*, **22**(6), 831–840.

Lau, K. M., C. P. Chang, and S. H. Shen, 1988: Seasonal and intraseasonal climatology of summer monsoon rainfall over East Asia. *Mon. Wea. Rev.*, **116**, 18–37.

Li, C. Y., J. T. Wang, S. Z. Lin, and H. R. Cho, 2004: The relationship between Asian summer monsoon activity and northward jump of the upper westerly jet location. *Chinese J. Atmos. Sci.*, **28**(5), 641–658. (in Chinese)

Liang, X. Z., and W. C. Wang, 1998: Associations between China monsoon rainfall and tropospheric jets. *Quart. J. Roy. Meteor. Soc.*, **14**, 2597–2623.

Liang, X. Y., Y. M. Liu, and G. X. Wu, 2006: Roles of tropical and subtropical land-sea distribution and the Qinghai-Xizang Plateau in the formation of the Asian summer monsoon. *Chinese Journal Geophysics*, **49**(4), 983–992.

Liu, Y. M., G. X. Wu, H. Liu, and P. Liu, 1999a: The effect of spatially non-uniform heating on the formation and variation of subtropical high. Part III: Condensation heating and south Asia high and western pacific subtropical high. *Acta Meteorologica Sinica*, **57**(5), 525–538. (in Chinese)

Liu, Y. M., G. X. Wu, and H. Liu, 1999b: Disposal of negative orography in a spectral model and modeling of subtropical climate in East Asia. *Chinese J. Atmos. Sci.*, **23**(6), 652–662. (in Chinese)

Liu, Y. M., G. X. Wu, H. Liu, and P. Liu, 2001: Condensation heating of the Asian summer monsoon and the subtropical anticyclone in the Eastern Hemisphere. *Climate Dyn.*, **17**, 327–338.

Liu, Y. M., G. X. Wu, and R. C. Ren, 2004: Relation between the Subtropical Anticyclone and Diabatic Heating. *J. Climate*, **17**(4), 682–698.

Tao, S. Y., Y. J. Zhao, and X. M. Chen, 1958: The association between Mei-yu in East Asia and seasonal variation of the general circulation of atmosphere over Asia. *Acta Meteorologica Sinica*, **29**(2), 119–134. (in Chinese)

Wang, B., H. Wan, Z. Z. Ji, X. Zhang, R. C. Yu, Y. Q. Yu, and H. T. Liu, 2004: Design of a new dynamical core for global atmospheric models based on some efficient numerical methods. *Science in China* (A), **47**, 4–21.

Wang, Z. Z., G. X. Wu, P. Li, and T. W. Wu, 2005a: The development of GOALS/LASG AGCM and its global climatological features in climate simulation I—Influence of horizontal resolution. *Journal of*

Tropical Meteorology, **21**(3), 225–237. (in Chinese)

Wang, Z. Z., R. C. Yu, P. F. Wang, and G. X. Wu, 2005b: The development of GOALS/LASG AGCM and its global climatological features in climate simulation II—The increase of vertical resolution and its influences. *Journal of Tropical Meteorology*, **21**(3), 238–247. (in Chinese)

Wu, G. X., and Y. M. Liu, 2003: Summertime quadruplet heating pattern in the subtropics and the associated atmospheric circulation. *Geophys. Res. Lett.*, **30**, 1201–1204.

Wu, G. X., H. Liu, Y. C. Zhao, and W. P. Li, 1996: A nine-layer atmospheric general circulation model and its performance. *Adv. Atmos. Sci.*, **13**, 1–18.

Wu, T. W., G. X. Wu, Z. Z. Wang, and R. C. Yu, 2004a: Simulation of the mean state in the GOALS/LASG model. *Acta Meteorologica Sinica*, **62**(1), 20–29. (in Chinese)

Wu, T. W., G. X. Wu, and R. C. Yu, 2004b: The evaluation of the ENSO-Like interannual variation in the GOALS/LASG model. *Acta Meteorologica Sinica*, **62**(2), 155–166. (in Chinese)

Xie, P. P., and P. A. Arkin, 1997: Global precipitation: A 17-year monthly analysis based on gauge observation, satellite estimates, and numerical model output. *Bull. Amer. Meteor. Soc.*, **78**, 2539–2558.

Yanai, M., S. Esbensen, and J. H. Chu, 1973: Determination of bulk properties of tropical cloud clusters from large scale heat and moisture budgets. *J. Atmos. Sci.*, **30**, 611–627.

Yang, S., K. M. Lau, and K. M. Kim, 2002: Variations of the East Asian jet stream and Asian-Pacific-American winter climate anomalies. *J. Climate*, **15**, 306–325.

Yeh, D. Z., and B. Z. Zhu, 1955: The onset of the transitional seasons in the Far East from the viewpoint of the general circulation. *Acta Meteorologica Sinica*, **26**, 71–87. (in Chinese)

Yeh, D. Z., S. Y. Tao, and M. C. Li, 1958: The abrupt change of circulation over Northern Hemisphere during June and October. *Acta Meteorologica Sinica*, **29**(4), 250–263. (in Chinese)

Yin, M. T., 1949: A synoptic-aerological study of the onset of the summer monsoon over India and Burma. *J. Meteor.*, **6**, 393–400.

Yu, R. C., 1994: Application of a shape-preserving advection scheme to the moisture equation in an E-grid regional forecast model. *Adv. Atmos. Sci.*, **11**(4), 479–490.

Yu, R. C., B. Wang, and T. J. Zhou, 2004: Tropospheric cooling and summer monsoon weakening trend over East Asia. *Geophys. Res. Lett.*, **31**, L22212, doi:10.1029/2004GL021270.

Zhang, Q., G. X. Wu, and Y. F. Qian, 2002: The bimodality of the 100 hPa South Asia High and its relationship to the climate anomaly over East Asia in summer. *J. Meteor. Soc. Japan*, **80**(4), 733–744.

Zhang, Y. C., and L. L. Guo, 2005: Relationship between the simulated East Asian westerly jet biases and seasonal evolution of rainbelt over eastern China. *Chinese Science Bulletin*, **50**, 1503–1508.

Zhang, Y. C., X. Y. Kuang, W. D. Guo, and T. J. Zhou, 2006: Seasonal evolution of the upper-tropospheric westerly jet core over East Asia. *Geophys. Res. Lett.*, **33**, L11708, doi:10.1029/2006GL026377.

Zhou, T. J., and Z. X. Li, 2002: Simulation of the east Asian summer monsoon by using a variable resolution atmospheric GCM. *Climate Dyn.*, **19**, 167–180.

Zhou, T. J., and R. C. Yu, 2005: Atmospheric water vapor transport associated with typical anomalous summer rainfall patterns in China. *J. Geophys. Res.*, **110**, D08104, doi: 10.1029/2004JD005413.

Zhou, T. J., and R. C. Yu, 2006: Twentieth century surface air temperature over China and the globe simulated by coupled climate models. *J. Climate*, **19**(22), 5843–5858.

Zhou, T. J., and Coauthors, 2005a: *The Atmospheric General Circulation Model SAMIL and the Associated Coupled Model FGOALS_s*. 1st ed, China Meteorological Press, 288pp.

Zhou, T. J., and Coauthors, 2005b: The climate system model FGOALS_s using LASG/IAP spectral AGCM SAMIL as its atmospheric component. *Acta Meteorologica Sinica*, **63**(5), 702–715. (in Chinese)